nature medicine

Stem cells act through multiple mechanisms to benefit mice with neurodegenerative metabolic disease

Jean-Pyo Lee[1,2,12], Mylvaganam Jeyakumar[3,12], Rodolfo Gonzalez[1], Hiroto Takahashi[1,11], Pei-Jen Lee[1], Rena C Baek[4], Dan Clark[1], Heather Rose[1], Gerald Fu[1], Jonathan Clarke[1], Scott McKercher[1], Jennifer Meerloo[1], Franz-Josef Muller[1,5], Kook In Park[6], Terry D Butters[3], Raymond A Dwek[3], Philip Schwartz[7], Gang Tong[1,8], David Wenger[9], Stuart A Lipton[1,8], Thomas N Seyfried[4], Frances M Platt[3] & Evan Y Snyder[1,2,10]

Intracranial transplantation of neural stem cells (NSCs) delayed disease onset, preserved motor function, reduced pathology and prolonged survival in a mouse model of Sandhoff disease, a lethal gangliosidosis. Although donor-derived neurons were electrophysiologically active within chimeric regions, the small degree of neuronal replacement alone could not account for the improvement. NSCs also increased brain β-hexosaminidase levels, reduced ganglioside storage and diminished activated microgliosis. Additionally, when oral glycosphingolipid biosynthesis inhibitors (β-hexosaminidase substrate inhibitors) were combined with NSC transplantation, substantial synergy resulted. Efficacy extended to human NSCs, both to those isolated directly from the central nervous system (CNS) and to those derived secondarily from embryonic stem cells. Appreciating that NSCs exhibit a broad repertoire of potentially therapeutic actions, of which neuronal replacement is but one, may help in formulating rational multimodal strategies for the treatment of neurodegenerative diseases.

Stem cells, particularly neural stem cells (NSCs), possess a range of actions that are potentially therapeutic. One of these, functional neuronal replacement[1], may in fact be complemented or even eclipsed by others, such as the delivery of therapeutic gene products synthesized inherently by the stem cell[2–6], the blunting of toxic components of the microenvironment[5,7] and the replacement of the multiple neural elements that define a given CNS region. Furthermore, NSCs may synergize with other therapies.

We investigated these assumptions in a mouse model of Sandhoff disease[8], a rapidly progressive, monogenic disorder resulting from an abnormal accumulation of ganglioside within lysosomes throughout the central nervous system (CNS). A deletion of the β-chain of β-hexosaminidase (Hex) results in deficiencies in the isoenzymes HexA (αβ) and HexB (ββ). Children with the disease have severe mental retardation and motor dysfunction, and death typically occurs in infancy. This and other lysosomal storage diseases (LSDs) are also characterized by a prominent injurious inflammatory signature[9–11]. One obstacle to treatment is the inability to circumvent the blood-brain barrier in order to deliver persistent, effective levels of therapeutic molecules to the affected areas. Furthermore, because of the multiple pathophysiological processes involved, more than one strategy is required.

To model NSC behavior, we first used mouse NSCs (mNSCs) and then human NSCs (hNSCs) isolated directly from the human fetal CNS ('primary' hNSCs), as well as those derived *in vitro* from human embryonic stem cells (hESCs) ('secondary' hNSCs). This study was designed to determine how NSCs respond in a model of neurogenetic degenerative disease and to determine whether both sources of hNSCs are equally efficacious. We subsequently studied whether NSC actions could be used rationally and effectively in a collaborative or synergistic manner with other strategies, using oral substrate reduction therapy as a case in point.

RESULTS

Transplanted mNSCs prolong life and improve motor deficits

The Sandhoff disease mouse typically becomes symptomatic by 90 d of age and dies between 114–130 d, depending on strain and/or cage conditions. We began our study using a stable, clonal population of dependably engraftable *lacZ*-expressing mNSCs. These were taken from a well-characterized clone, C17.2, because its enhanced yet

[1]Stem Cell & Regeneration Program, Center for Neuroscience and Aging Research, Burnham Institute for Medical Research, La Jolla, California 92037, USA. [2]Department of Pediatrics, University of California San Diego, School of Medicine, La Jolla, California 92093, USA. [3]Department of Biochemistry, Glycobiology Institute, University of Oxford, Oxford OX1 3QU, UK. [4]Biology Department, Boston College, Chestnut Hill, Massachusetts 02467, USA. [5]Zentrum für Integrative Psychiatrie, Kiel 24105, Germany. [6]Department of Pediatrics, Yonsei University College of Medicine, Seoul 120-749, Korea. [7]Children's Hospital of Orange County Research Institute, Orange, California 92826, USA. [8]Department of Neurosciences, University of California San Diego, School of Medicine, La Jolla, California 92093, USA. [9]Department of Neurology, Jefferson Medical College, Philadelphia, Pennsylvania 19107, USA. [10]San Diego Consortium for Regenerative Medicine, La Jolla, California 92037, USA. [11]Present address: Janelia Farm Research Campus, Ashburn, Virginia 20147, USA. [12]These authors contributed equally to this work. Correspondence should be addressed to E.Y.S. (esnyder@burnham.org) or F.M.P. (frances.platt@pharm.ox.ac.uk).

Received 28 March 2006; accepted 16 January 2007; published online 11 March 2007; doi:10.1038/nm1548

constitutively self-regulated[2] expression of stemness genes[14–18] permits its cells to be efficiently grown in sufficiently large, homogenous and viable quantities to ensure reproducible patterns of integration[12,13]. Hence, we were able to compare large numbers of mice while eliminating interpassage/intertrial variability in engraftment, migration, differentiation, potency, species compatibility, and cell number and survival. Having established baseline expectations, we then transitioned to using mNSCs isolated from Rosa mice as neurospheres, which, although less homogenous, were expanded with mitogens alone (**Supplementary Methods** online). Ultimately, we used hNSCs (both from the CNS and from hESCs).

When mNSCs were transplanted into the forebrain and cerebellum of newborn mice with Sandhoff disease (*Hexb*$^{-/-}$), their physical appearance and coat condition (a sign of well-being) were sustained in comparison to untreated age-matched mice (**Fig. 1a**). Symptom onset was delayed and lifespan was prolonged up to 170 d, an ~70% improvement (**Fig. 1b**). By 90 d, untreated *Hexb*$^{-/-}$ mice showed severely impaired motor function and coordination[19]. We assessed the motor function of age-matched mNSC-transplanted *Hexb*$^{-/-}$ mice by rotarod performance and the righting reflex test (**Supplementary Fig. 1** online) and found that these mice performed significantly better ($P < 0.001$; *t*-test) than untreated *Hexb*$^{-/-}$ mice, suggesting preserved motor function. Transplanted mice showed no symptoms for up to 16 weeks. We did not see adverse effects or reduced lifespan in any of the transplanted mice.

We obtained similarly beneficial results when we transplanted mNSCs isolated and expanded as neurospheres[2] from a Rosa 26 mouse (**Fig. 1c,d**). As a negative control, we transplanted fibroblasts, which failed to migrate from the lateral ventricles; motor function and survival curves were indistinguishable from those of untreated *Hexb*$^{-/-}$ mice (**Fig. 1b–d** and **Supplementary Fig. 1**).

NSCs engraft widely and generate neurons

We next explored potential mechanisms underlying this improvement. Might the benefit derive from replacing dysfunctional mutant neurons with a sufficient number of wild-type NSC-derived neurons? Because the relative contribution of donor cells to particular regions might help address this question, we first examined the distribution of engraftment. After implantation into neonatal cerebral ventricles alone, donor-derived cells were evident throughout the forebrain (with a predilection for cortical and subcortical regions); however, hindbrain engraftment was less robust (**Fig. 1e** and **Supplementary Figs. 2** and **3** online). When transplantation into the neonatal cerebellum[2,20] was piggy-backed onto the intraventricular regime, the median onset of symptoms was delayed by an additional 20 d, and median lifespan was extended by an additional 18 d. The extent of engraftment in the cerebellar cortex (predominantly the internal granular layer) was similar to that in the cerebral cortex (**Fig. 1f**). Such results were consistent with a simple cell replacement model wherein an added benefit was derived both from the increased number of wild-type cells afforded by a second transplant and from the specific location of those cells, given that cerebellar pathology contributes substantially to the symptomatology in Sandhoff disease. To discern the degree to which the replacement of mutant with wild-type neural cells, particularly neurons, might be contributory, we created maximally chimeric regions by implanting mNSCs (both

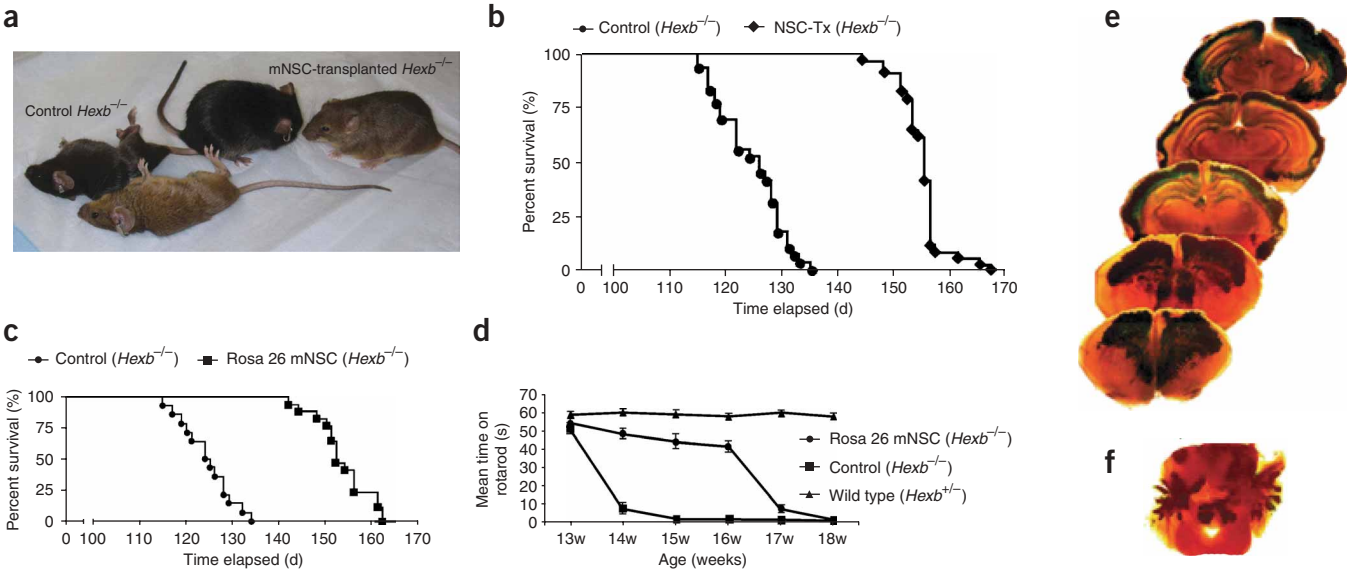

Figure 1 Transplantation of mNSCs into the brains of *Hexb*$^{-/-}$mice prolongs life, delays symptom onset and preserves motor function. (**a**) At a time when untreated *Hexb*$^{-/-}$ mice were moribund, mNSC-transplanted *Hexb*$^{-/-}$ mice were asymptomatic. (**b**) Kaplan-Meyer curves of the survival of mNSC-transplanted *Hexb*$^{-/-}$ mice ($n = 43$) compared with untreated *Hexb*$^{-/-}$ control mice ($n = 57$) ($P < 0.0001$, log rank test). Data were obtained using mNSCs from clone C17.2. (**c**) Lifespan of mouse neurosphere–transplanted *Hexb*$^{-/-}$ mice ($n = 16$) was similarly prolonged compared to that of untreated *Hexb*$^{-/-}$ mice ($n = 14$) ($P < 0.0001$, log rank test). (**d**) Motor function test of neurosphere-transplanted *Hexb*$^{-/-}$ mice compared with that of untreated *Hexb*$^{-/-}$ control mice ($P < 0.001$, *t*-test). Data represent mean ± s.e.m; $n = 9$ wild-type mice. Motor function deteriorated at 13 weeks in untreated control *Hexb*$^{-/-}$ mice ($n = 14$) but was delayed to at least 16 weeks, with a more gradual decline between 16 and 18 weeks, in neurosphere-transplanted *Hexb*$^{-/-}$ mice (Rosa 26 mNSC-Tx *Hexb*$^{-/-}$, $n = 16$). (**e**) Representative 1-mm-thick semiserial coronal sections through the forebrain of an adult *Hexb*$^{-/-}$ mouse transplantated at birth with *lacZ*-expressing mNSCs into the cerebral ventricles, showing widely disseminated integration of blue X-gal^{+} donor-derived cells. (**f**) As in **e** but showing coronal section through cerebellum of adult *Hexb*$^{-/-}$ mouse transplantated as newborn into the external germinal layer. Similar cerebral and cerebellar distributions were obtained whether NSCs were from mouse clone C17.2 (here), ROSA mouse neurospheres, human neuroectoderm or hESCs (**Supplementary Figs. 1–4** and **Supplementary Table 1**).

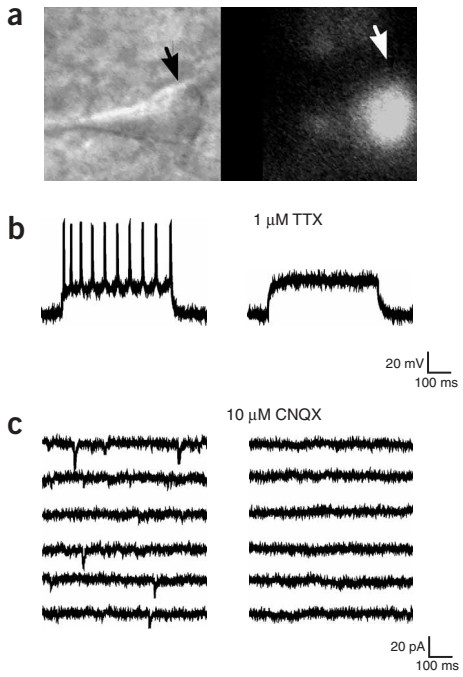

Figure 2 mNSCs differentiate into a range of neural cell types in the *Hexb*$^{-/-}$ mouse cortex, including electrophysiologically active neurons. NSC-derived neurons, like the Neuronal nuclei (NeuN)-immunopositive cells shown in **Supplementary Figures 2** and **4**, were further analyzed for electrophysiological properties suggestive of neuronal differentiation and integration. (**a**) Infrared (left) and fluorescence (right) images of a cortical slice from a 2-month-old *Hexb*$^{-/-}$ mouse engrafted with eGFP-expressing mNSCs *in utero*. These mNSCs were isolated from fetal wild-type mice and expanded as neurospheres in bFGF (Methods). A living transplanted mNSC-derived cell in the *Hexb*$^{-/-}$ cortex was identified by its eGFP signal. Arrows at left and right indicate the same cell. (**b**) Action potentials, in a donor-derived neuron, induced by depolarization (left) and inhibited by 1 μM TTX (right). (**c**) Spontaneous activity was recorded from a donor mNSC–derived neuron at a holding potential of –75 mV in the presence of 1 μM TTX and 1 mM Mg^{2+} (left); the miniature excitatory postsynaptic currents were abolished by 10 μM CNQX. Taken together, these findings indicated mediation by AMPA receptors (right).

mitogen-expanded neurospheres and cells from clone C17.2) into the *Hexb*$^{-/-}$ CNS *in utero* (via the ventricular zone) on embryonic day 13.5 (E13.5) during active cortical neurogenesis[21]. At 2 months of age, we immunocytochemically assessed these mNSC-derived cells, which integrated widely throughout the neuraxis[12], for their expression of neural cell type–specific markers (**Supplementary Fig. 4** online). Confocal microscopic analysis assaying the expression of immunomarkers suggested that they differentiated into multiple neural cell types, including neurons (4.19 ± 0.6%), astroglia (38.4 ± 2.3%), undifferentiated progenitors (54.41 ± 3.1%) and oligodendroglia (1.04 ± 0.07%) (**Supplementary Fig. 4** and **Supplementary Table 1** online). The nestin-expressing cells did not coexpress glial fibrillary acidic protein (GFAP), suggesting that they were neural progenitors and not reactive astrocytes. We obtained similar results when the mNSCs were transplanted at birth except that few, if any, cortical neurons were observed (the proportion of astrocytes was slightly higher: ~43%) (**Fig. 1e**,**f** and **Supplementary Fig. 2**).

As the expression of immunomarkers alone is not sufficient to establish the identity of a neural cell, we used live cortical slices from adult *Hexb*$^{-/-}$ brains that had been transplanted *in utero* with mNSCs engineered *ex vivo* to express enhanced green fluorescent protein (eGFP); eGFP expression would allow us to identify and patch-clamp neurons derived from implanted mNSCs and determine whether they were indeed electrophysiologically active. We then identified living donor-derived cells using fluorescence infrared differential interference contrast (IR-DIC) microscopy (**Fig. 2a**). Under current-clamp conditions, injecting depolarizing currents produced a burst of spikes from eGFP^{+} donor-derived cells (**Fig. 2b**). The spikes were inhibited by 1 μM tetrodotoxin (TTX) (**Fig. 2b**), confirming the presence of action potentials. We also recorded spontaneous miniature postsynaptic currents at a holding potential of –75 mV in the presence of TTX (1 μM) and Mg^{2+} (1 mM) (**Fig. 2c**). All miniature postsynaptic currents were abolished by 6-cyano-7-nitroquinoxaline-2,3-dione (CNQX) (10 μM), a specific AMPA receptor antagonist (**Fig. 2c**). Therefore, we concluded that transplanted mNSCs developed into electrophysiologically active neurons. However, the improvement in motor function and lifespan were similar whether mNSCs were administered prenatally (during cortical neurogenesis, when more cortical neurons were generated) or neonatally (when few, if any, cortical neurons were produced). Therefore, we concluded that neuronal replacement was not the predominant mechanism of rescue and, consequently, investigated additional mechanisms.

NSCs increase Hex and diminish GM2/GA2

NSCs expressed normal levels of Hex constitutively, secreting fully assembled active HexA (αβ) and HexB (ββ) isoenzymes. For example, mNSC lysates had specific Hex activity, 2.89 ± 0.02 μmol/mg/h, which compared favorably with the total Hex-specific activity present in whole-brain preparations from asymptomatic wild-type mice (1.45 ± 0.06 μmol/mg/h). HexS (αα) constitutes <2% of total Hex activity; in fact, most Hex activity was divided between HexA (one-third) and HexB (two-thirds) intracellularly. This ratio persists in the extracellular compartment, with 10% of intracellular Hex being secreted[21,22].

Because NSCs are able to cross-correct Hex-deficient neural cells *in vitro*[2], we hypothesized that constitutively Hex-expressing NSCs may similarly be compensating for Hex deficiencies *in vivo* by producing the missing enzyme and cross-correcting host cells. Hex activity in the mNSC-engrafted *Hexb*$^{-/-}$ cerebrum was nearly 5% of that in wild-type cells (**Fig. 3a**). In well-engrafted regions (such as certain regions of cortex; **Supplementary Fig. 2**), the donor-host cell ratio was 1:10, yielding 28% of normal Hex activity in the vicinity of the most dense cellular concentrations; as little as 2–5% of wild-type Hex activity is known to be sufficient to restore normal metabolism[23]. These ratios (and hence their relationship to enzyme expression) were replicated using hNSCs (see below; also **Supplementary Table 1**).

An indicator of the physiological significance of enzyme reconstitution is its impact on the glycosphingolipid (GSL) gangliotriaosylceramide (GA2) and monosialoganglioside (GM2) storage in *Hexb*$^{-/-}$ mice[23]. We used immunochemistry to assess GSL distribution and content in the cerebral cortex of *Hexb*$^{-/-}$ mice transplanted at birth with mNSCs and also measured this directly by high-performance thin-layer chromatography (HPTLC). Biochemically, GM2 was 40% lower in transplanted *Hexb*$^{-/-}$ mice (NSC-Tx-*Hexb*$^{-/-}$) than in non-transplanted age-matched *Hexb*$^{-/-}$ mice (**Fig. 3b**,**c**). GM2 storage was abundant in the 2-month-old nontransplanted *Hexb*$^{-/-}$ brain (**Fig. 3d**) but was virtually undetectable in the same region of the age-matched transplanted *Hexb*$^{-/-}$ brain (**Fig. 3e**). GA2 content was also significantly reduced in the transplanted *Hexb*$^{-/-}$ brain (**Fig. 3f**,**g**). GM2 and GA2 were undetected in normal mouse brains. The impact on GM2/GA2 storage was replicated below using hNSCs.

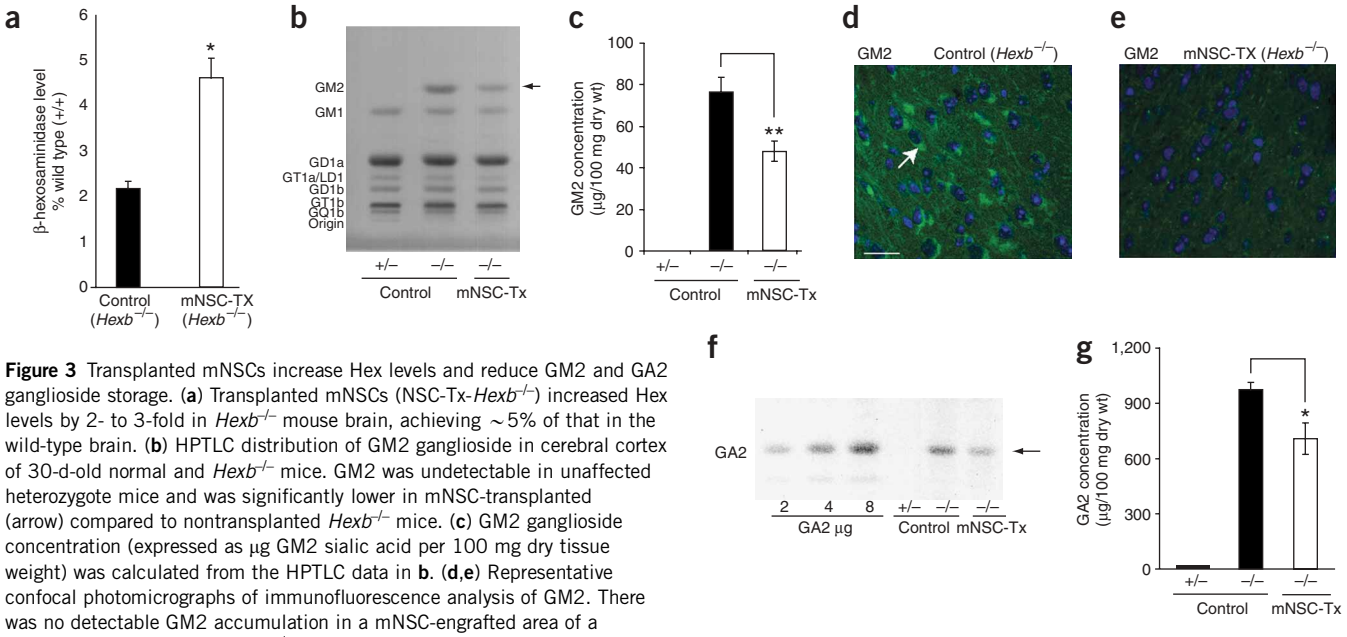

Figure 3 Transplanted mNSCs increase Hex levels and reduce GM2 and GA2 ganglioside storage. (**a**) Transplanted mNSCs (NSC-Tx-*Hexb*$^{-/-}$) increased Hex levels by 2- to 3-fold in *Hexb*$^{-/-}$ mouse brain, achieving ~5% of that in the wild-type brain. (**b**) HPTLC distribution of GM2 ganglioside in cerebral cortex of 30-d-old normal and *Hexb*$^{-/-}$ mice. GM2 was undetectable in unaffected heterozygote mice and was significantly lower in mNSC-transplanted (arrow) compared to nontransplanted *Hexb*$^{-/-}$ mice. (**c**) GM2 ganglioside concentration (expressed as μg GM2 sialic acid per 100 mg dry tissue weight) was calculated from the HPTLC data in **b**. (**d**,**e**) Representative confocal photomicrographs of immunofluorescence analysis of GM2. There was no detectable GM2 accumulation in a mNSC-engrafted area of a 2-month-old transplanted *Hexb*$^{-/-}$ mouse brain, whereas substantial amounts of GM2 (green immunoreaction product, arrow) were noted in the same region of an age-matched, nontransplanted *Hexb*$^{-/-}$ mouse brain. Cells were visualized by blue nuclear 4,6-diamidino-2-phenylindole (DAPI) staining. (**f**) HPTLC distribution of GA2 in the cortex of normal and *Hexb*$^{-/-}$ mice at 30 d, showing that GA2 content was undetectable in the unaffected heterozygote mice and was substantially lower in mNSC-transplanted (arrow) compared to nontransplanted *Hexb*$^{-/-}$ mice. (**g**) GA2 concentration, expressed as μg GA2 per 100 mg of dry tissue weight, was calculated from the standard curve of purified GA2 in **f**. Values expressed as mean ± s.e.m.; 4–5 independent cortical samples were analyzed per group. $^{**}P < 0.01$, $^{*}P < 0.05$ (two-tailed *t*-test).

Reduced microglial activation with NSC transplantation

Abundant microglial activation and macrophage infiltration is a hallmark of Sandhoff disease pathogenesis[9–11]. As NSCs have an anti-inflammatory influence when transplanted into the traumatized brain[5] and spinal cord[24], we wondered whether this action might occur in such neurodegenerative conditions as the Sandhoff disease brain. We used microglia/macrophage activation markers to monitor CNS inflammation in the mNSC-engrafted *Hexb*$^{-/-}$ brain (**Fig. 4**), specifically in the primary motor cortex (M1) (**Fig. 4a**), a region efficiently engrafted by mNSCs (**Fig. 1e** and **Supplementary Figs. 2–4**). CD11b immunoreactivity was abundant in the unengrafted *Hexb*$^{-/-}$ cortex (**Fig. 4a**). In age-matched (15-week-old) transplanted

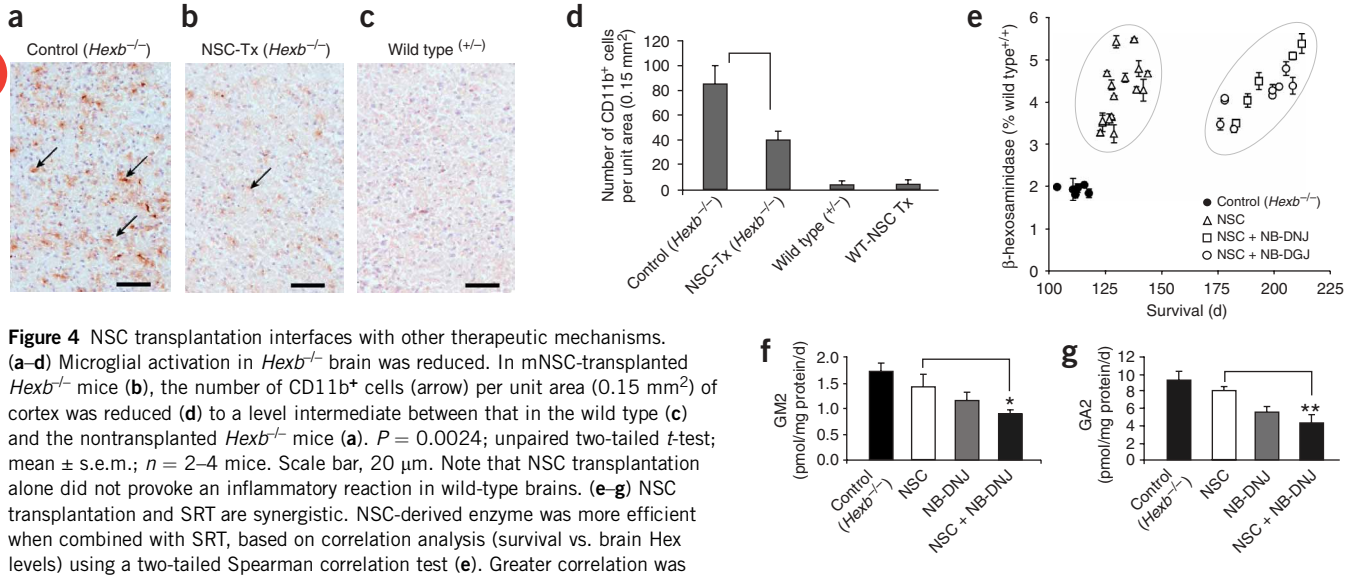

Figure 4 NSC transplantation interfaces with other therapeutic mechanisms. (**a**–**d**) Microglial activation in *Hexb*$^{-/-}$ brain was reduced. In mNSC-transplanted *Hexb*$^{-/-}$ mice (**b**), the number of CD11b^{+} cells (arrow) per unit area (0.15 mm^2) of cortex was reduced (**d**) to a level intermediate between that in the wild type (**c**) and the nontransplanted *Hexb*$^{-/-}$ mice (**a**). $P = 0.0024$; unpaired two-tailed *t*-test; mean ± s.e.m.; $n = 2$–4 mice. Scale bar, 20 μm. Note that NSC transplantation alone did not provoke an inflammatory reaction in wild-type brains. (**e**–**g**) NSC transplantation and SRT are synergistic. NSC-derived enzyme was more efficient when combined with SRT, based on correlation analysis (survival vs. brain Hex levels) using a two-tailed Spearman correlation test (**e**). Greater correlation was observed in the combination therapy group ($P < 0.0001$) compared to the NSC monotherapy group ($P < 0.01$) for the same enzyme level. Cerebral NSC transplantation increased enzyme content beyond that in untreated *Hexb*$^{-/-}$ control brains, and addition of SRT shifted that cluster (left-hand oval) further rightward (right-hand oval), signifying longer survival with the same enzyme levels (doubling survival in some mice). (Cerebellum was not transplanted in these experiments.) (**f**,**g**) NSC + NB-DNJ therapy reduced GSL storage in *Hexb*$^{-/-}$ mouse brains below that in untreated *Hexb*$^{-/-}$ brains or *Hexb*$^{-/-}$ brains receiving monotherapy. GM2 and GA2 (standardized against mouse age) are expressed as pmol/mg protein (mean ± s.e.m., unpaired two-tailed *t*-test; $n = 3$–4). $^{*}P < 0.002$; $^{**}P < 0.0004$.

mice, staining in region-matched sections was reduced (**Fig. 4b**) to a level intermediate between that in wild-type (**Fig. 4c,d**) and untreated *Hexb*$^{-/-}$ (**Fig. 4a**) brains. Using additional macrophage/microglial markers (for example, F4/80 and CD68) yielded similar results (data not shown). NSCs of human origin similarly diminished microgliosis (**Supplementary Fig. 5** online). As in previous reports[9–11], lymphocyte infiltration (assessed by the T cell–specific immunomarkers CD4 and CD8) was not a characteristic of Sandhoff disease, even in late-stage mouse brains (**Supplementary Fig. 5**). Also noteworthy is that mNSCs transplanted into wild-type mouse brains, although an allograft, did not provoke a reactive microglial reaction (**Fig. 4d**) or other evidence of inflammation or immunorejection.

Substrate reduction synergizes with NSC transplantation

Can the efficiency of the cross-corrective enzyme supplied by the NSCs be enhanced by reducing the amount of substrate to be metabolized? Imino sugars, specifically *N*-butyldeoxynojirimycin (NB-DNJ) or *N*-butyldeoxygalactonojirimycin (NB-DGJ), inhibit GSL biosynthesis and reduce storage in some LSD mouse models[19,25–28], an intervention termed substrate reduction therapy (SRT). When transplantation of mNSCs into neonatal cerebrum was combined with NB-DNJ or NB-DGJ administration (starting at 6 weeks of age), *Hexb*$^{-/-}$ mouse survival increased by 67–71% ($P < 0.0001$; log rank test)—that is, prolonging life by as long as 215 d (a doubling of lifespan for some mice; (**Supplementary Fig. 6** online). Implants into the cerebellum were not combined with cerebral transplants in these experiments.

Statistical analysis of survival data using the bootstrap procedure[29] indicated synergy. The null and alternative hypotheses are H_0 : SQ = 1 vs. H_1: SQ < 1, respectively. SQ is the synergy quotient: (NSC monotherapy effect + SRT monotherapy effect)/(NSC + SRT combination therapeutic effect). SQ1 assesses the effect of NSC + NB-DNJ, and SQ2 assesses the effect of NSC + NB-DGJ. The estimated SQs (0.86974 and 0.88635, respectively) were both significantly less than 1, indicating synergy. The NSC + NB-DNJ combination therapy yielded 13% synergy ($P = 0.018$), and NSC + NB-DGJ yielded 11% synergy ($P = 0.047$) (compare **Fig. 1b** and **Supplementary Fig. 6**).

In mNSC-treated mice, survival correlated with the level of Hex activity in the brain ($P < 0.01$), but this survival was greater (that is, reached greater significance: $P < 0.0001$) when combined with SRT (**Fig. 4e**). A two-tailed Spearman correlation test confirmed the interaction of these two independent therapeutic modalities. Therefore, NSCs alone significantly increased baseline enzyme whereas the addition of SRT (**Fig. 4e**) shifted that cluster further rightward, indicating enhanced survival (despite no change in enzyme level) and more efficient use of that enzyme (due to the reduction in its substrate burden). SRT alone had limited impact, because of residual small amounts of HexS, which is less metabolically active.

We also observed an improvement in motor function in the combination therapy group ($P < 0.001$) (**Supplementary Fig. 6**): the onset age of dysfunction was significantly delayed compared to the

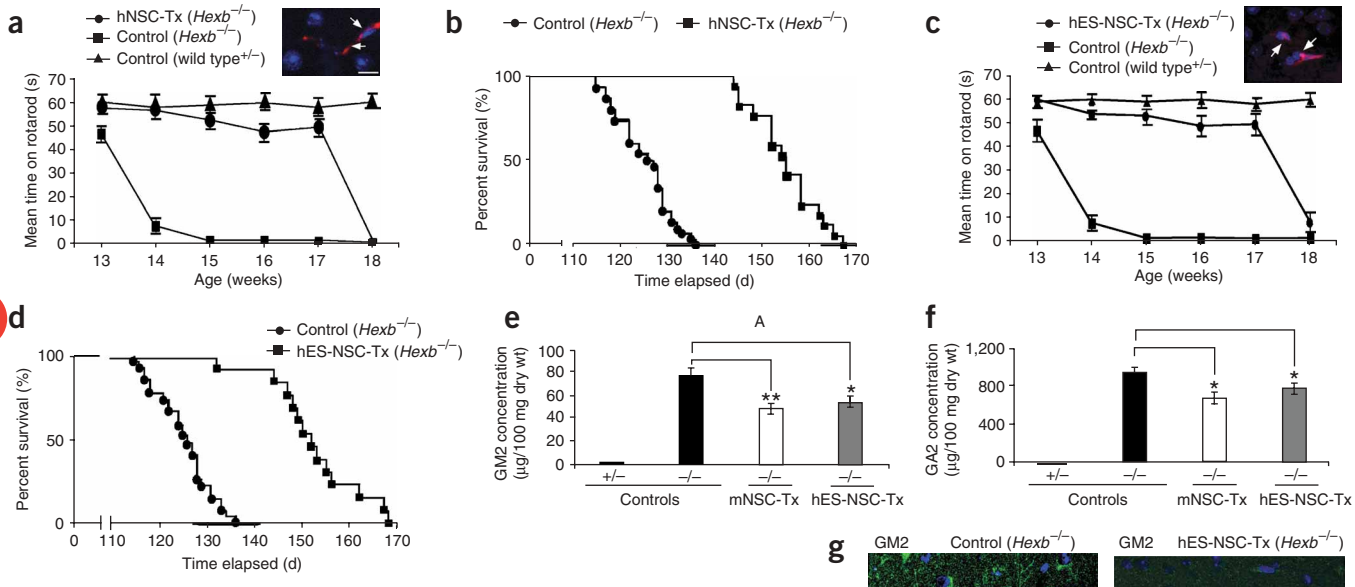

Figure 5 Both 'primary' (CNS-derived) and 'secondary' (hESC-derived) human NSC transplantation benefit *Hexb*$^{-/-}$ mice. (**a**,**b**) Transplantation (Tx) of primary hNSCs (hNSC-Tx) delayed the motor deterioration ($n = 41$) compared with that of nontransplanted control *Hexb*$^{-/-}$ mice ($n = 33$) (mean ± s.e.m.; $P < 0.001$, *t*-test) and prolonged their lifespan by ~40% ($n = 37$) compared to that of nontransplanted *Hexb*$^{-/-}$ mice ($n = 42$) ($P < 0.0001$; log rank test). Inset in **a** shows engrafted hNSC-derived cells, identified by their immunoreactivity (red) to an antibody against human mitochondria (hMito) (arrows), in the cortex of a 4-month-old *Hexb*$^{-/-}$ mouse (nuclei stained blue by DAPI). Scale bar, 10 μm. (**c**,**d**) Transplantation of secondary hNSCs (hES-NSCs) similarly preserved the rotarod function ($n = 41$) otherwise lost in nontransplanted *Hexb*$^{-/-}$ mice ($n = 33$) and prolonged their survival ($P < 0.0001$; log rank test). Inset in **c** as per inset in **a** but for hMito^{+} hES-NSCs. (**e**,**f**) Neonatally transplanted hES-NSCs reduced GM2 and GA2 in the cortices of 30-d-old *Hexb*$^{-/-}$ mice compared to age-matched nontransplanted *Hexb*$^{-/-}$ mice. Data in age-matched mNSC-transplanted *Hexb*$^{-/-}$ mice are provided for comparison. Untransplanted heterozygous mice served as normal controls (4–6 independent samples per group). $^{**}P < 0.01$, $^{*}P < 0.05$ (two-tailed *t*-test). (**g**) GM2 immunoreactivity (green, arrow) was abundant in the cortex of a nontransplanted 2-month-old *Hexb*$^{-/-}$ mouse (representative photomicrograph) but was nondetectable in the same region of an age-matched hES-NSC-engrafted *Hexb*$^{-/-}$ mouse. Nuclei stained by DAPI. Scale bar, 25 μm.

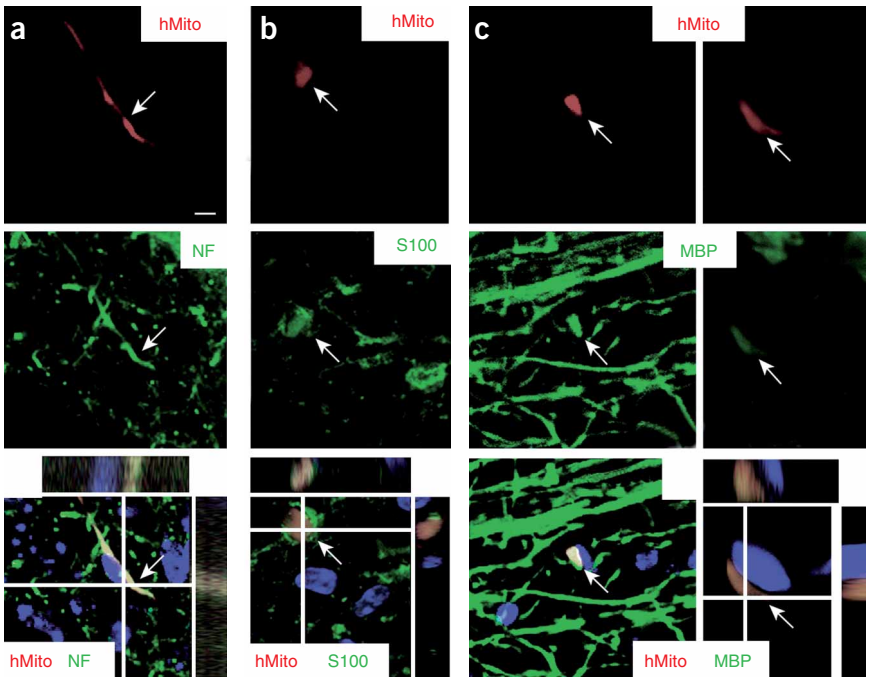

Figure 6 hNSCs (derived from hESCs) stably engrafted in the *Hexb*$^{-/-}$ mouse cortex for at least 5.5 months after neonatal transplantation, differentiating into cells expressing neuronal and glial markers. (**a**–**c**) Representative donor-derived cells, recognized by their immunoreactivity to hMito (red) (top), coexpress neuronal markers (such as neurofilament (NF)) and glial markers (S-100β and myelin basic protein (MBP)) (middle). Merged images show blue DAPI nuclear staining to identify all cells in the field (bottom). Each merged image is also shown as an orthogonal projection composed of 9–16 optical *Z*-planes of thickness 0.5–1 μm. Arrows in each panel of a given column indicate the same cell. (**c**) Donor-derived MBP^{+} cells are shown both at low power (left) to highlight their integration within a white tract recognized as a field of MBP-expressing cells, as well as at higher magnification (right) to confirm their MBP expression via orthogonal views. No non-neural cell types or tumors were seen ($n = 41$). No immunosuppression was used. Scale bar, 25 μm.

untreated ($P < 0.001$), NSC-alone or SRT-alone groups. The combined therapy reduced GM2 and GA2 storage by an additional 50% relative to NSCs alone (**Fig. 4f,g**). Wild-type mice were not adversely affected under any condition (**Supplementary Fig. 6**). Therefore, adding an oral pharmacologic agent increased the enzyme action of NSCs without requiring genetic manipulation[21,30].

Insights from mNSCs may extend to NSCs of human origin

Primary (CNS-derived) hNSCs, transplanted at birth into the forebrain and cerebellum of *Hexb*$^{-/-}$ mice significantly delayed the onset of motor impairment—by 1 month ($P < 0.001$, *t*-test; **Fig. 5a**)—with no deterioration until after 17 weeks, and significantly prolonged mouse lifespan—by 1.5 months, to 170 d (**Fig. 5b**). This means that disease onset was delayed by 1 additional week and lifespan extended by 1 additional week compared with that in mNSC-transplanted groups (**Fig. 1a–d** and **Supplementary Fig. 1**). We confirmed the presence of hNSC-derivatives throughout the *Hexb*$^{-/-}$ mouse brain by immunostaining with an antibody to human mitochondria (**Fig. 5a** and **Supplementary Fig. 3**).

Similarly transplanted secondary (hESC-derived) hNSCs had a comparable effect on motor function (**Fig. 5c**) and lifespan (**Fig. 5d**), with survival extended to 170 d. We detected hESC-derived hNSCs in the CNS for at least 5.5 months after transplantation (**Fig. 5c**). No tumors or non-neural cell types developed in >20 SCID mice or in >100 *Hexb*$^{-/-}$ mice transplanted with these cells, nor was survival compromised in either group. (The hESCs were maintained in a defined culture system that would be compatible with clinical use.)

Using high-performance thin layer chromatography (HPTLC) (**Fig. 5e,f**) and immunocytochemistry (**Fig. 5g**), we determined that GM2 and GA2 storage was reduced by 30% ($P < 0.01$; two-tailed test) in hNSC-transplanted brains as compared to that in nontransplanted, age-matched *Hexb*$^{-/-}$ brains. This was comparable to the effects seen with mNSC transplants (**Fig. 5e,f**). These levels correlated with survival and preservation of motor function (**Fig. 5a–d**). Microgliosis, too, was diminished (**Supplementary Fig. 5**), as reported above with mNSCs (**Fig. 4**). Although engrafted hESC-derived hNSCs differentiated into cells with neuronal (**Fig. 6a**), astroglial (**Fig. 6b**) and oligodendroglial (**Fig. 6c**) lineages (**Supplementary Table 1**), as did mNSCs (**Supplementary Fig. 4**), the impact of donor wild-type cells on host cells and the host milieu predominated over neuronal replacement in improving the outcome in Sandhoff disease (**Supplementary Table 1**). The hNSCs persisted long term in the *Hexb*$^{-/-}$ mouse brain and exerted their effect without requiring immunosuppression.

DISCUSSION

Transplanted NSCs migrated extensively throughout the *Hexb*$^{-/-}$ mouse brain, disseminating the cross-correcting enzyme, reducing ganglioside storage and inflammation, and creating some chimeric regions in which mutant cells were replaced with wild-type cells. The small percentage of donor-derived cells that were neurons probably had the smallest impact, even though these were electrophysiologically active. However, the cells with greatest impact were probably the non-neuronal progeny of these NSCs, which, by serving as chaperone cells for host (and donor-derived) neurons, constitutively supplied physiologically relevant amounts of cross-corrective Hex; this could then be taken up by host cells via their mannose-6-phosphate receptor, thereby reducing ganglioside storage.

In addition to, or as a consequence of, this action, the NSCs reduced inflammation. These combined functions probably forestalled disease onset, slowed disease progression, preserved motor function and substantially extended lifespan. That such findings pertain regardless of NSC species, source or method of expansion and propagation suggests that multiple homeostatic actions may be inherent to a stem cell's fundamental behavior. No immunosuppression was required nor was an immunoinflammatory reaction provoked. hNSCs were equally efficacious and safe whether isolated directly from the CNS or from hESCs *in vitro*. (There is interest in the stem cell field in discerning whether these two methods for deriving ostensibly the 'same cell' (for example, the hNSC) are, in fact, equally efficacious in a head-to-head comparison.)

Inflammation, though often underappreciated and of an etiology that is not well understood, plays a significant pathophysiological role in LSDs. Given that some anti-inflammatory strategies have been useful to treat individuals with Sandhoff disease even in the absence of enzyme replacement or GM2 storage reduction[9–11,24,31,32], reduced brain inflammation itself could be a component of the NSCs' impact. In other words, whereas reduced inflammation may be attributed to reduced ganglioside storage, these data also raise the possibility that NSCs may inherently exert an anti-inflammatory influence in this degenerative disease (as they are postulated to do in other more classic neuroinflammatory conditions[5,24,33]).

Why were mice with Sandhoff disease not permanently 'cured'? Once deterioration began, the rate patterned that of nontransplanted mice, albeit with a slope shifted significantly to the right. Sandhoff and others[23,34] theorized that the pattern of deterioration, which is similar to that seen in other neurodegenerative diseases, suggests that once a certain 'critical threshold' of storage is attained, the cells or their connections become rapidly dysfunctional. In our *Hexb*$^{-/-}$ mice transplanted once as newborns, this threshold hypothesis might hold: it is possible that as the mice grew to adulthood, the proliferation of new mutant host cells ultimately outstripped the influence of the finite number of engrafted wild-type postmitotic NSCs. Readministration of NSCs may prevent the donor to host cell ratio from declining below a level that achieves a critical threshold of cross-corrective enzyme (our data suggest that a 1:10 ratio in key functional regions is desirable and that it probably should not be less than 1:140; **Supplementary Table 1**).

Sandhoff disease also affects the brainstem, spinal cord and, to a lesser extent, the peripheral nervous system (PNS); these are regions that cannot be optimally treated using only an intracranial transplant, and hence a fall below the critical threshold is possible. Just as the impact of intraventricular implantation was improved by the addition of cerebellar engraftment, it is likely that intracranial transplantation needs to be combined with additional strategies to reach these areas. Bone marrow transplantation (BMT) can correct peripheral manifestations, although it is poorly suited for enzyme and neural cell replacement in the CNS (ref. 2).

Keeping ganglioside storage below its critical threshold can be achieved by increasing donor-cell distribution (probably requiring additional invasive procedures) and/or by enhancing the quantity of enzyme produced by the NSCs (probably requiring genetic manipulation[21,30,35]). Here we tested, as proof of concept, a more benign approach: increasing the efficiency of the NSC-mediated Hex activity already present by reducing the amount of substrate to be metabolized. This strategy, which sought to synergize with the stem cell's repertoire of constitutive actions, was achieved by simply adding an oral pharmacologic agent. SRT is typically effective only when at least a small amount of enzyme is already present (as is the case in the late-onset and slowly progressive forms of metabolic diseases). Where no enzyme is present, as in most infantile forms, the impact of SRT is expected to be limited and it is unlikely to be effective. However, when combined with a constant source of the appropriate lysosomal enzyme (even at low levels), as provided by stably integrated wild-type NSCs, SRT use in these more virulent conditions becomes credible. In some mice with Sandhoff disease, this synergy doubled lifespan—to 215 d (**Fig. 4**).

In summary, there is a growing appreciation that in most CNS diseases, including those of monogenic etiology, the multiple pathophysiological processes that coalesce to create symptomatology and degeneration preclude relying on a single therapeutic strategy to restore function. This idea parallels our growing appreciation of the multifaceted actions of the NSC. Although functional neuronal replacement[36–39] has received the most attention (even though it is the most difficult of stem cell actions), it can be complemented—and, in some conditions, eclipsed, as we suggest here—by a range of other stem cell actions that nevertheless exert various homeostatic forces. Given the complexities of CNS development, preserving established circuitry is as important as, and probably safer and more tractable than, attempting to reconstruct new connections. In many of these infantile disorders, if multimodal (including stem cell) treatment is instituted early enough to effect rescue, minimal cell replacement and circuit reconstruction may be demanded of the NSC.

METHODS

Mice. Sandhoff founder mice were generated by deletion of the Hex β-subunit[8]. Experiments were carried out on two *Hexb*$^{-/-}$ mouse lines with different degrees of C57BL6 backcrossing and 14-d differences in life expectancy, hence controlling for differences related to background strain. We analyzed outcomes separately within each strain and then normalized for comparisons. Genotypes were determined on tail DNA. The animal experiments were approved by the Animal Research Committee at the Burnham Institute for Medical Research and University of Oxford.

NSC and hESC cultures. Details are in **Supplementary Methods**. Briefly, we used four NSC sources, as described below.

1. A stable, clonal population of engraftable *lacZ*-expressing mNSCs (clone C17.2) that had a history of successful mouse transplantation[3,5,13] and also fulfilled the operational definition of a stem cell[12,13] (including enhanced expression of stemness genes[13–15,17,18,40] that are constitutively self-regulated[2], facilitating expansion of homogenous monolayers).
2. mNSCs isolated as neurospheres from the telencephalon of E10.5 Rosa 26 mice and maintained[2] with bFGF (20 ng/ml) + heparin (8 μg/ml) in N2 medium. Neurospheres are heterogenous and may vary from passage to passage[41].
3. 'Primary' hNSCs isolated from the telencephalic ventricular zone (VZ) of late first-trimester human fetal cadavers[2,42]. Following a serial growth factor selection procedure[1,2,43], the hNSCs were maintained in serum-free medium containing bFGF (20 ng/ml), heparin (8 μg/ml) and leukemia inhibitory factor (LIF) (10 ng/ml).
4. 'Secondary' hNSCs derived *in vitro* from hESCs (US National Institutes of Health line WA09) maintained under defined, feeder-free culture conditions. To direct these hESCs toward hNSCs, we used documented procedures based on exposure to retinoic acid (10 μM), with minor modifications[37,44,45].

Transplantation. Details are in **Supplementary Methods**. Guided by transillumination of the newborn mouse head, we gently expelled 2 μl of the NSC suspension (5×10^4 NSCs/μl in PBS)[3,21], through a glass micropipette, into each cerebral ventricle of anesthetized *Hexb*$^{-/-}$ pups (and unaffected littermate controls). This allowed the NSCs access to the subventricular germinal zone[12]. For neonatal cerebellar transplants[2,20], we transilluminated the hindbrain and injected 2 μl of the NSC suspension into the external germinal layer of each of the hemispheres and the vermis. For *in utero* NSC transplantation[21],we subjected isofluorane-anesthetized *Hexb*$^{+/-}$ female mice, impregnated by *Hexb*$^{-/-}$ males, to ventral laparotomy at E13.5. We then injected them with the NSC suspension (1 μl), through the transilluminated uterine wall into the embryos' telencephalic vesicles, allowing the NSCs access to the VZ.

Histological and immunocytochemical assessment. For immunocytochemical analysis of 20-μm paraformaldehyde-fixed coronal cryosections, we used routine procedures (refs. 1,2,43 and **Supplementary Methods**). *Escherichia coli* β–galactosidase (β-gal) in the mNSCs allowed reliable identification of donor-derived cells by 5-bromo-4-chloro-3-indolyl-β-D-galactoside (X-gal) histochemistry or by β-gal–specific immunocytochemistry[2,3,5]. We identified hNSCs by human-specific antibodies[1,42]. We detected cell type–specific antigens with the following primary antibodies: nestin for immature neural progenitors; neurofilament, NeuN and microtubule associated protein-2 for neurons; GFAP, S-100β for astroglia; CNPase and myelin basic protein for oligodendroglia. We

assessed CNS inflammation in part with antibodies to markers of microglia/macrophage activation (such as F4/80, CD68 and CD11b)[11] and examined lymphocyte infiltration with antibodies to CD4 and CD8. Quantitation adhered to unbiased stereological techniques[46,47].

Confocal microscopy. We acquired images using a Bio-Rad MRC 1024 equipped with a single photon Kr/Ar laser and a Bio-Rad Radiance 2100MP equipped with a multiphoton laser. Image pixel resolution was 1024 × 1024, and images were acquired sequentially to negate channel cross-talk. Negative and positive control images were taken with the same settings. Each merged image was visualized using orthogonal projections composed of 9–16 optical *Z*-planes of thickness 0.5–1 μm.

Electrophysiology. We performed whole-cell patch-clamp recordings on fluorescent donor-derived cells in live cortical slices obtained acutely from the brains of *Hexb*$^{-/-}$ mice 9 weeks after *in utero* transplantation[48]. Briefly, we engineered donor mNSCs (isolated from E10.5 mouse telencephalon) to express eGFP by transduction *ex vivo* with a replication-defective retrovirus (pcMMP-MLV based). We obtained living coronal slices (400 μm thick) from decapitated adult mice using a vibrating microtome in chilled, gassed artificial cerebrospinal fluid (ACSF) followed by incubation in gassed ACSF at 30 °C. After placing the slices in a submerged chamber at 25 °C, we obtained whole-cell recordings in current- or voltage-clamp mode from donor-derived cells identified by their eGFP fluorescence. Details are in **Supplementary Methods**.

Enzyme activity assay. Hex activity was assayed routinely using 4-methylumbelliferyl-*N*-acetyl-β-D-glucosaminide as the substrate (as in ref. 49).

GSL analysis. Brain GSLs were extracted and quantified using HPTLC as detailed previously[27,50].

Behavioral testing. As detailed in **Supplementary Methods**, we evaluated motor function by rotarod performance tested twice weekly for 10-week-old-mice until they could no longer walk. Thereafter, we used the righting reflex test. The mice were killed when they could no longer right themselves within 20 s of being laid on their side. See **Supplementary Methods** for details of horizontal bar-crossing test[19].

SRT. *Hexb*$^{-/-}$ mice were treated with NB-DNJ or NB-DGJ as a dry admix with powdered mouse chow (600 mg/kg/d, Oxford GlycoSciences)[26] beginning at 6 weeks of age. Untreated mice were fed a control powder diet on the same schedule as the treated groups.

Note: Supplementary information is available on the Nature Medicine website.

ACKNOWLEDGMENTS

Supported by National Tay-Sachs and Allied Diseases Association (NTSAD), Late-Onset Tay-Sachs Foundation, Children's Neurobiological Solutions, A-T Children's Project, Barbara Anderson Foundation for Brain Repair, Project ALS, March of Dimes, Hunter's Hope, Lysosomal Storage Disease Research Consortium, Neurosurgery Neuroscience Consortium, Division of Neurosurgery at the University of California, San Diego, National Institute of General Medicine, National Eye Institute, National Institute of Neurological Diseases and Stroke, National Institute of Child Health and Human Development, Korean Ministry of Science and Technology, Medical Research Council and the University of Oxford.

COMPETING INTERESTS STATEMENT

The authors declare no competing financial interests.

Published online at http://www.nature.com/naturemedicine
Reprints and permissions information is available online at http://npg.nature.com/reprintsandpermissions

1. Imitola, J. *et al.* Directed migration of neural stem cells to sites of CNS injury by the stromal cell-derived factor 1alpha/CXC chemokine receptor 4 pathway. *Proc. Natl. Acad. Sci. USA* **101**, 18117–18122 (2004).
2. Flax, J.D. *et al.* Engraftable human neural stem cells respond to developmental cues, replace neurons, and express foreign genes. *Nat. Biotechnol.* **16**, 1033–1039 (1998).
3. Snyder, E.Y., Taylor, R.M. & Wolfe, J.H. Neural progenitor cell engraftment corrects lysosomal storage throughout the MPS VII mouse brain. *Nature* **374**, 367–370 (1995).
4. Martinez-Serrano, A., Fischer, W. & Bjorklund, A. Reversal of age-dependent cognitive impairments and cholinergic neuron atrophy by NGF-secreting neural progenitors grafted to the basal forebrain. *Neuron* **15**, 473–484 (1995).
5. Park, K.I., Teng, Y.D. & Snyder, E.Y. The injured brain interacts reciprocally with neural stem cells supported by scaffolds to reconstitute lost tissue. *Nat. Biotechnol.* **20**, 1111–1117 (2002).
6. Givogri, M.I. *et al.* Oligodendroglial progenitor cell therapy limits central neurological deficits in mice with metachromatic leukodystrophy. *J. Neurosci.* **26**, 3109–3119 (2006).
7. Kondo, Y., Wenger, D.A., Gallo, V. & Duncan, I.D. Galactocerebrosidase-deficient oligodendrocytes maintain stable central myelin by exogenous replacement of the missing enzyme in mice. *Proc. Natl. Acad. Sci. USA* **102**, 18670–18675 (2005).
8. Sango, K. *et al.* Mice lacking both subunits of lysosomal beta-hexosaminidase display gangliosidosis and mucopolysaccharidosis. *Nat. Genet.* **14**, 348–352 (1996).
9. Wada, R., Tifft, C.J. & Proia, R.L. Microglial activation precedes acute neurodegeneration in Sandhoff disease and is suppressed by bone marrow transplantation. *Proc. Natl. Acad. Sci. USA* **97**, 10954–10959 (2000).
10. Myerowitz, R. *et al.* Molecular pathophysiology in Tay-Sachs and Sandhoff diseases as revealed by gene expression profiling. *Hum. Mol. Genet.* **11**, 1343–1350 (2002).
11. Jeyakumar, M. *et al.* Central nervous system inflammation is a hallmark of pathogenesis in mouse models of GM1 and GM2 gangliosidosis. *Brain* **126**, 974–987 (2003).
12. Park, K. *et al.* Acute injury directs the migration, proliferation, and differentiation of solid organ stem cells: evidence from the effect of hypoxia-ischemia in the CNS on clonal "reporter" neural stem cells. *Exp. Neurol.* **199**, 156–178 (2006).
13. Parker, M.A. *et al.* Expression profile of an operationally-defined neural stem cell clone. *Exp. Neurol.* **194**, 320–332 (2005).
14. Cartwright, P. *et al.* LIF/STAT3 controls ES cell self-renewal and pluripotency by a Myc-dependent mechanism. *Development* **132**, 885–896 (2005).
15. Light, W., Vernon, A.E., Lasorella, A., Iavarone, A. & LaBonne, C. *Xenopus* Id3 is required downstream of Myc for the formation of multipotent neural crest progenitor cells. *Development* **132**, 1831–1841 (2005).
16. Takahashi, K. & Yamanaka, S. Induction of pluripotent stem cells from mouse embryonic and adult fibroblast cultures by defined factors. *Cell* **126**, 663–676 (2006).
17. Maragakis, N.J. *et al.* Glial restricted precursors protect against chronic glutamate neurotoxicity of motor neurons in vitro. *Glia* **50**, 145–159 (2005).
18. Murphy, M.J., Wilson, A. & Trumpp, A. More than just proliferation: Myc function in stem cells. *Trends Cell Biol.* **15**, 128–137 (2005).
19. Jeyakumar, M. *et al.* Delayed symptom onset and increased life expectancy in Sandhoff disease mice treated with N-butyldeoxynojirimycin. *Proc. Natl. Acad. Sci. USA* **96**, 6388–6393 (1999).
20. Rosario, C.M. *et al.* Differentiation of engrafted multipotent neural progenitors towards replacement of missing granule neurons in meander tail cerebellum may help determine the locus of mutant gene action. *Development* **124**, 4213–4224 (1997).
21. Lacorazza, H.D., Flax, J.D., Snyder, E.Y. & Jendoubi, M. Expression of human beta-hexosaminidase alpha-subunit gene (the gene defect of Tay-Sachs disease) in mouse brains upon engraftment of transduced progenitor cells. *Nat. Med.* **2**, 424–429 (1996).
22. Hultberg, B., Isaksson, A., Nordstrom, M. & Kjellstrom, T. Release of beta-hexosaminidase isoenzymes in cultured human fibroblasts. *Clin. Chim. Acta* **216**, 73–79 (1993).
23. Conzelmann, E. & Sandhoff, K. Partial enzyme deficiencies: residual activities and the development of neurological disorders. *Dev. Neurosci.* **6**, 58–71 (1983).
24. Teng, Y.D. *et al.* Functional recovery following traumatic spinal cord injury mediated by a unique polymer scaffold seeded with neural stem cells. *Proc. Natl. Acad. Sci. USA* **99**, 3024–3029 (2002).
25. Tifft, C.J. & Proia, R.L. Stemming the tide: glycosphingolipid synthesis inhibitors as therapy for storage diseases. *Glycobiology* **10**, 1249–1258 (2000).
26. Platt, F.M. *et al.* Prevention of lysosomal storage in Tay-Sachs mice treated with N-butyldeoxynojirimycin. *Science* **276**, 428–431 (1997).
27. Kasperzyk, J.L. *et al.* N-butyldeoxygalactonojirimycin reduces neonatal brain ganglioside content in a mouse model of GM1 gangliosidosis. *J. Neurochem.* **89**, 645–653 (2004).
28. Andersson, U. *et al.* Improved outcome of N-butyldeoxygalactonojirimycin-mediated substrate reduction therapy in a mouse model of Sandhoff disease. *Neurobiol. Dis.* **16**, 506–515 (2004).
29. Davison, A.C. & Hinkley, D.V. *Bootstrap Methods and Their Application.* (Cambridge Univ. Press, Cambridge, UK, 2003).
30. Pellegatta, S. *et al.* The therapeutic potential of neural stem/progenitor cells in murine globoid cell leukodystrophy is conditioned by macrophage/microglia activation. *Neurobiol. Dis.* **21**, 314–323 (2006).
31. Wu, Y.P. & Proia, R.L. Deletion of macrophage-inflammatory protein 1 alpha retards neurodegeneration in Sandhoff disease mice. *Proc. Natl. Acad. Sci. USA* **101**, 8425–8430 (2004).
32. Jeyakumar, M. *et al.* NSAIDs increase survival in the Sandhoff disease mouse: synergy with N-butyldeoxynojirimycin. *Ann. Neurol.* **56**, 642–649 (2004).
33. Pluchino, S. *et al.* Injection of adult neurospheres induces recovery in a chronic model of multiple sclerosis. *Nature* **422**, 688–694 (2003).
34. Gravel, R.A. *et al.* The GM2 gangliosidoses. in *The Metabolic and Molecular Bases of Inherited Disease* (eds. Scriver, C.R., Beaudet, A.L., Valle, D. & Sly, W.S.) 3827–3876 (McGraw-Hill, New York, 2001).

35. Cachon-Gonzalez, M.B. *et al.* Effective gene therapy in an authentic model of Tay-Sachs-related diseases. *Proc. Natl. Acad. Sci. USA* **103**, 10373–10378 (2006).
36. Roy, N.S. *et al.* Functional engraftment of human ES cell-derived dopaminergic neurons enriched by coculture with telomerase-immortalized midbrain astrocytes. *Nat. Med.* **12**, 1259–1268 (2006).
37. Zhang, S.C., Wernig, M., Duncan, I.D., Brustle, O. & Thomson, J.A. *In vitro* differentiation of transplantable neural precursors from human embryonic stem cells. *Nat. Biotechnol.* **19**, 1129–1133 (2001).
38. Svendsen, C.N. *et al.* Long-term survival of human central nervous system progenitor cells transplanted into a rat model of Parkinson's disease. *Exp. Neurol.* **148**, 135–146 (1997).
39. Muotri, A.R., Nakashima, K., Toni, N., Sandler, V.M. & Gage, F.H. Development of functional human embryonic stem cell-derived neurons in mouse brain. *Proc. Natl. Acad. Sci. USA* **102**, 18644–18648 (2005).
40. Knoepfler, P.S., Cheng, P.F. & Eisenman, R.N. N-myc is essential during neurogenesis for the rapid expansion of progenitor cell populations and the inhibition of neuronal differentiation. *Genes Dev.* **16**, 2699–2712 (2002).
41. Reynolds, B.A. & Rietze, R.L. Neural stem cells and neurospheres–re-evaluating the relationship. *Nat. Methods* **2**, 333–336 (2005).
42. Schwartz, P.H. *et al.* Isolation and characterization of neural progenitor cells from post-mortem human cortex. *J. Neurosci. Res.* **74**, 838–851 (2003).
43. Ourednik, V. *et al.* Segregation of human neural stem cells in the developing primate forebrain. *Science* **293**, 1820–1824 (2001).
44. Carpenter, M.K. *et al.* Enrichment of neurons and neural precursors from human embryonic stem cells. *Exp. Neurol.* **172**, 383–397 (2001).
45. Reubinoff, B.E. *et al.* Neural progenitors from human embryonic stem cells. *Nat. Biotechnol.* **19**, 1134–1140 (2001).
46. Coggeshall, R.E. & Lekan, H.A. Methods for determining numbers of cells and synapses: a case for more uniform standards of review. *J. Comp. Neurol.* **364**, 6–15 (1996).
47. Guillery, R.W. & Herrup, K. Quantification without pontification: choosing a method for counting objects in sectioned tissues. *J. Comp. Neurol.* **386**, 2–7 (1997).
48. Stuart, G.J., Dodt, H.U. & Sakmann, B. Patch-clamp recordings from the soma and dendrites of neurons in brain slices using infrared video microscopy. *Pflugers Arch.* **423**, 511–518 (1993).
49. Wenger, D.A. & Williams, C. Screening for lysosomal disorders. in *Techniques in Diagnostic Human Biochemical Genetics. A Laboratory Manual* (ed. Hommes, F.A.) 587–617 (Wiley-Liss, New York, 1991).
50. Neville, D.C. *et al.* Analysis of fluorescently labeled glycosphingolipid-derived oligosaccharides following ceramide glycanase digestion and anthranilic acid labeling. *Anal. Biochem.* **331**, 275–282 (2004).